

Integration of Inverse Supercritical Fluid Extraction and Miniaturized Asymmetrical Flow Field-Flow Fractionation for the Rapid Analysis of Nanoparticles in Sunscreens

David Müller,^{*,†,‡,§,¶,||} Margarida Nogueira,[†] Stefano Cattaneo,[†] Florian Meier,[§] Roland Drexel,[§] Catia Contado,^{||} Antonella Pagnoni,^{||} Tjerk de Vries,[⊥] Dror Cohen,[#] Meital Portugal-Cohen,[#] and Andrew deMello^{‡,Ⓛ}

[†]Centre Suisse d'Electronique et de Microtechnique (CSEM), Bahnhofstrasse 1, 7302 Landquart, Switzerland

[‡]Institute for Chemical and Bioengineering, Department for Chemistry and Applied Biosciences, ETH Zürich, Vladimir-Prelog-Weg 1, 8093 Zürich, Switzerland

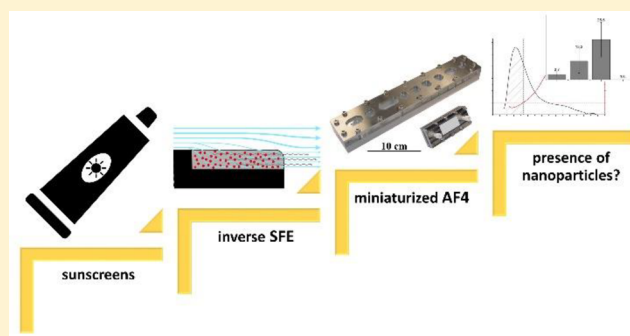
[§]Postnova Analytics GmbH, Max-Planck-Strasse 14, 86899 Landsberg am Lech, Germany

^{||}Department of Chemical and Pharmaceutical Sciences, University of Ferrara, Via L. Borsari 46, 44121 Ferrara, Italy

[⊥]Feyecon Carbon Dioxide Technologies, Rijnkade 17a, 1382 GS Weesp, The Netherlands

[#]AHAVA Dead Sea Laboratories, 1 Arava Street, 70150 Lod, Israel

ABSTRACT: We report the use of inverse supercritical fluid extraction (SFE) and miniaturized asymmetrical flow field-flow fractionation (mAF4) for the preparation and subsequent analysis of titanium dioxide nanoparticles in model and commercial sunscreens. The approach allows for the fast and reliable fractionation and sizing of TiO₂ nanoparticles and their quantitation in commercial products. This new method represents a powerful and efficient tool for the verification of nanoparticle content in a wide range of matrixes, as demanded by recently introduced regulatory requirements. Furthermore, the use of carbon dioxide as an environmentally friendly solvent is in line with the increasing need for ecologically compatible analytical techniques.



Recently introduced European Union regulations on cosmetic products require that all ingredients present in the form of nanomaterials be clearly indicated as such in the list of ingredients.¹ This requirement calls for the development of comprehensive analytical procedures to ensure manufacturer compliance. The analysis of nanoparticles in complex media, consisting of a complex multicomponent matrix,² is a multifaceted challenge involving multiple component processes for sample pretreatment, separation of the engineered nanoparticles (ENPs) from the matrix, separation of nanoparticles on the basis of their size, and chemical analysis. To this end, Wagner et al. recently presented such a categorization in a generic sample preparation scheme for inorganic ENPs within complex matrixes.³ Such generic procedures, which also integrate appropriate quality criteria to confirm the applicability of the suggested methods, are urgently needed for standardized and systematic development of processes for the separation and analysis of ENPs in complex matrixes. In this respect, the most pressing needs are the development of new analytical techniques for extraction, cleanup, and separation with a view to improving analytical speed, sensitivity, and specificity.⁴ One of the most challenging components of the Wagner scheme is

the reduction in complexity of the ENP containing sample, either through extraction of nanoparticles from their environment or through simplification of the matrix by removal of excipients that interfere with subsequent analysis. There are several techniques that are frequently used for the isolation of nanoparticles from such matrixes, including acid digestion (assisted by heat, sonication, or microwaves),^{3,5–8} colloidal extraction,^{3,9} or various treatments with organic solvents.^{7,10,11} However, all these processes are complex and time-consuming. Many also completely destroy the particulate nature of the samples, rendering particle size analysis impossible, or have a considerable environmental impact due to the extensive use of harmful solvents.^{12,13} Accordingly, the simplification of sample preparation workflows as well as a reduction in solvent requirements, are highly desirable for the analysis of nanoparticle-containing samples.

To this end, we present a novel method for the analysis of TiO₂ nanoparticles in commercial sunscreens, comprising two

Received: November 2, 2017

Accepted: February 7, 2018

Published: February 7, 2018

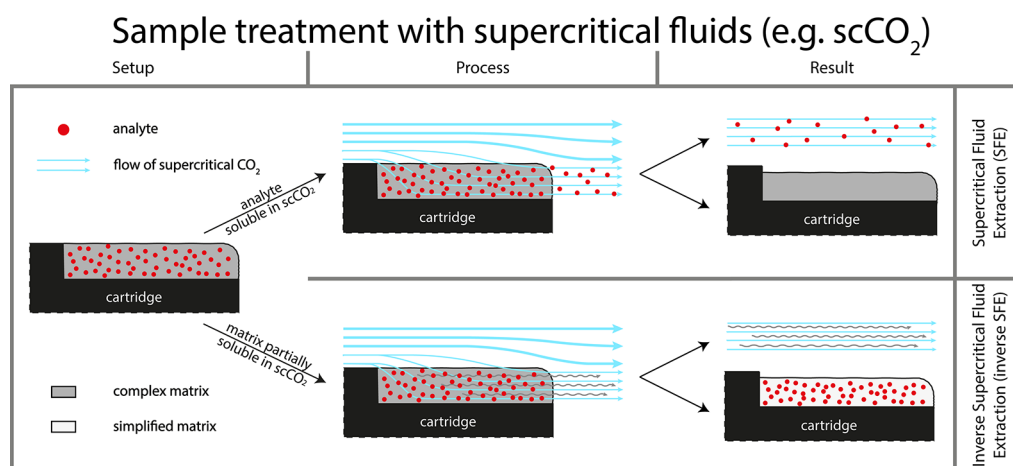


Figure 1. Principles of SFE (top) and inverse SFE (bottom). The setup used for both processes is identical, the primary difference lying in the selection of analyte and matrix and whether the substance of interest is accordingly extracted or left within the simplified matrix.

analytical procedures. We herein propose the use of inverse supercritical fluid extraction (SFE) to simplify complex matrixes containing ENPs while maintaining their particulate nature. To date, the technique of inverse SFE has primarily been used for the isolation of nonpolar pharmaceutical formulations from polar analytes.^{13–15} In a recent publication, we presented proof-of-concept experiments that suggested the utility of the technique as a sample pretreatment tool for nanoparticle-containing samples. Specifically, a single model sunscreen was treated and subsequently analyzed by asymmetrical flow field-flow fractionation (AF4) in addition to UV and MALS (multiangle light scattering) detectors and the use of more sophisticated transmission electron microscopy (TEM) analysis.¹⁶ In the present work, we aim to provide a thorough quantitative analysis of several model and commercial sunscreens loaded with ENPs at varying concentrations. In addition to the measurement of processed materials using mAF4, the ENP content was also analyzed using element-specific tools such as inductively coupled mass spectrometry (ICP-MS) and inductively coupled plasma atomic emission spectroscopy (ICP-AES). Field-flow fractionation methods are ideal for such measurements due to the gentle forces used to induce analyte retention and prevent particle alteration.¹⁷ Crucially, the miniaturized AF4 platform reduces both processing times and eluent consumption.¹⁸

92 ■ MATERIALS AND METHODS

93 **Samples. Titanium Dioxide Nanoparticle Standards.** A
94 titanium dioxide (TiO₂)-nanoparticle dispersion, AERODISP
95 W 740 X (40% w/w, EVONIK Industries, Hanau, Germany)
96 was diluted and prepared according to a protocol described
97 elsewhere¹⁶ to yield a final particle concentration of 0.2 mg/
98 mL.

99 **Model Sunscreen.** The novel sample preparation method
100 was initially applied to three complex sunscreen models
101 containing different TiO₂ nanoparticle concentrations. Creams
102 were produced individually according to protocols described
103 elsewhere.¹⁶ In the final step, 0.5, 2.5, and 12.5% w/w of a
104 AERODISP W 740 X TiO₂ nanoparticle dispersion (40% w/w,
105 EVONIK Industries, Essen, Germany), as well as the excipients
106 Dow Corning 1503 (Dow Corning Corporation, Midland, MI,
107 United States) and Euxyl PE 9010 (Schülke & Mayr GmbH,
108 Norderstedt, Germany) were added to each cream, resulting in

a TiO₂ particle concentration of 0.2, 1.0, and 5.0% w/w, 109
110 respectively. All creams were homogenized for 5 min at 4000
111 rpm before being loaded into tubes and stored at room
112 temperature.

113 **Commercial Sunscreens.** Five different commercial creams
114 were used to assess our sample preparation method: one cream
115 with a sun protection factor (SPF) of 15 (NiveaCream15), two
116 creams of different brands with a SPF of 30 (GarnierCream30
117 and NiveaCream30), one cream with an SPF of 50
118 (CoopCream50), and a sun protection spray with an SPF of
119 30 (SherpaSpray30). The first three samples contain TiO₂
120 nanoparticles listed as an ingredient according to European
121 Union legislation, whereas the latter two do not list any
122 nanoparticles as ingredients.

123 **Sample Treatment.** Supercritical fluids are well-suited for
124 extraction processes due to their minimal surface tension, low
125 viscosities, and gas-like diffusivities, which allow for thorough
126 sample penetration while maintaining the structure of the
127 residual material.¹³ The most obvious choice for the current
128 application is supercritical carbon dioxide (scCO₂) because
129 almost all chemical excipients found in emulsion-based
130 cosmetic products are highly soluble in CO₂. scCO₂ is
131 chemically inert¹⁹ as well as being nontoxic and nonflam-
132 mable²⁰ and is commonly used in the extraction of small and/
133 or nonpolar molecules from natural materials.^{21–24} In this
134 regard, common applications include the extraction of essential
135 oils from herbs and spices,^{25,26} the removal of caffeine from
136 coffee beans,^{27,28} and the extraction and analysis of
137 antioxidants, preservatives, and sunscreen agents in cosmet-
138 ics.^{29,30} In all these applications, however, the analyte itself is
139 soluble in CO₂, with SFE being used to dissolve and remove
140 the analyte from the matrix (upper panel of Figure 1). In this
141 work, however, inverse SFE is used to simplify the matrix by
142 removal of only unwanted components (see lower part of
143 Figure 1). Put simply, the supercritical fluid permeates the
144 matrix, dissolving fatty components and leaving behind a
145 simplified matrix. Once complete, any residual CO₂ is simply
146 removed by lowering the pressure below the critical threshold
147 and returning to ambient conditions. The remaining sample
148 material consists of the polar components of the matrix (e.g.,
149 thickening agents) along with any nanoparticles present.
150 Residue can be easily rewetted and subsequently dispersed in
151 an aqueous matrix for subsequent analysis.

152 **Supercritical CO₂ Sample Treatment.** Details of the
153 analytical method have been described previously,¹⁶ and thus,
154 only the conditions and experimental setup are described
155 herein. For our measurements, the sunscreen was placed on a
156 Teflon cartridge surrounded by a stainless-steel holder. The
157 Teflon part contained a small recess, forming in a cavity with
158 dimensions of 60 × 10 × 0.2 mm and accommodating 100 mg
159 of cream. To ensure a reproducible sample volume, excess
160 sunscreen was removed using a spatula. The Teflon cartridge
161 was then removed from its holder, weighed, and placed in a
162 custom-made extraction vessel. The setup was equipped with a
163 high-pressure CO₂ pump, a pressure/flow regulating system,
164 and a vertically mounted extraction vessel. A custom-made
165 support was used to place two cartridges at once in the
166 extraction vessel. Data indicated no significant difference
167 between each position; however, only the measurements from
168 one cartridge position (closer to the CO₂ inlet) are shown. The
169 sample was then subjected to a constant scCO₂ flow of 80 g
170 min⁻¹ for 30 min at 40 °C and 131 bar. After extraction, the
171 cartridge was removed and placed in a 15 mL tube for storage.
172 Before the measurement, 10 mL of a solution of 0.2% (v/v)
173 NovaChem (Postnova Analytics GmbH, Landsberg am Lech,
174 Germany) in ultrapure water (Milli-Q, Billerica, United States)
175 was added. NovaChem is a mixture of nonionic and ionic
176 detergents that helps prevent particle agglomeration. The tube
177 was vortexed and sonicated at maximum power (132 kHz) for
178 30 min using an ultrasonic bath (Ultrasonic Cleaner USC-THD/
179 HF, VWR, Radnor, Pennsylvania, United States) previously
180 cooled to a temperature of 25 °C to further reduce eventual
181 particle agglomerates. All extractions were performed in
182 triplicate ($n = 3$).

183 **Microwave Assisted Digestion.** Between 0.15 and 0.2 g of
184 each sample was deposited in a Teflon vessel (Milestone Inc.,
185 Shelton, United States), to which 6 mL of nitric acid (ultrapure
186 p.a. > 65%, Sigma-Aldrich S.R.L., Milano, Italy), 1 mL of H₂O₂
187 (30% RPE, Carlo Erba Reagents S.r.l., Cornaredo, Italy), and 3
188 mL of HF (39.5% RPE, Carlo Erba Reagents S.r.l., Cornaredo,
189 Italy) were added. The samples were then digested in the
190 microwave oven (Ethos 900 Milestone, rotor HPR 1000/6M,
191 Milestone Inc., Shelton, United States) according to the
192 following program: 1 min at 250 W and 120 °C, 1 min at 0
193 W and 120 °C, 5 min at 250 W and 140 °C, 4 min at 400 W
194 and 220 °C, 3 min at 550 W and 220 °C, 5 min at 300 W and
195 220 °C. The vessel was then left to cool for at least 10 min
196 before it was opened, and 1.5 g of boric acid (99.97% trace
197 metal basis, Sigma-Aldrich S.R.L., Milano, Italy) was added.
198 The solution was then returned into the microwave for 5 min at
199 300 W. Finally, the vessel was cooled to ambient temperature,
200 and the contents were transferred to a volumetric flask where
201 ultrapure water was added to reach the final volume of 50 mL.
202 All creams dissolved quickly with no visible residue; the final
203 solutions were clear and transparent. All digestions were
204 performed in triplicate ($n = 3$).

205 **Element-Specific Batch Analysis and Recovery Rate.** For
206 the batch-analysis of samples, two different element-specific
207 detectors were used, namely ICP-AES and ICP-MS. For the
208 evaluation of recovery rates, the detected concentrations were
209 compared to those of the samples prepared by direct
210 microwave-assisted digestion (without any treatment by inverse
211 SFE) followed by the corresponding element-specific method.
212 These procedures have previously been shown to allow
213 recovery rates of $98.2 \pm 2.2\%$ for the ICP-AES⁵ and $101 \pm$
214 2% for the ICP-MS.⁷

Inductively Coupled Plasma–Atomic Emission Spectrom-
215 **etry.** Titanium determinations were carried out on a 216
PerkinElmer Optima 3100 XL (PerkinElmer Italia S.p.A, 217
Milano, Italy) ICP-AES equipped with an axial torch, 218
segmented array charge-coupled device detector, and Low- 219
Flow GemCone nebulizer with cyclonic spray chamber for 220
sample introduction and choosing, among the several wave- 221
lengths, the readings at 337.279 nm. The plasma conditions 222
used were an RF power of 1350 W applied to the plasma and 223
flow rates of 15 L min⁻¹ for the plasma gas and 0.5 L min⁻¹ for 224
the auxiliary gas with a nebulizer gas flow of 0.65 L min⁻¹. The 225
sample uptake was 1.5 mL min⁻¹ for each of 3 replicate scans. 226
The diluted standard solutions were prepared from an 227
elemental standard solution (1000 mg L⁻¹ Ti, monoelement 228
standard solution, Carlo Erba, Italy). Titanium quantification 229
limits were evaluated each time from the calibration curves, and 230
the values ranged between 0.54–0.59 mg L⁻¹. 231

Inductively Coupled Plasma–Mass Spectrometry. Tita- 232
nium contents were also determined using an Agilent 7900 233
(Agilent Technologies, Santa Clara, United States) ICP-MS. 234
Sample introduction was carried out with a concentric glass 235
Micromist nebulizer, quartz glass spray chamber and a quartz 236
glass axial torch. A RF power of 1550 W and an argon gas flow 237
of 15 L min⁻¹ with a 0.9 L min⁻¹ auxiliary gas flow and a carrier 238
gas flow of 1.05 L min⁻¹ were used. The sample uptake flow 239
rate was 1.38 mL min⁻¹ with a stabilization time of 60 s. The 240
titanium isotopes were recorded with an integration time of 0.5 241
s. All measurements were performed in triplicate in He-mode to 242
remove polyatomic interferences by introducing a helium flow 243
of 4.3 mL min⁻¹ to the collision cell. The calibration was 244
performed with a multielemental standard solution of 1 mg L⁻¹ 245
titanium (CPAchem Ltd., Stara Zagora, Bulgaria), and a 246
detection limit of $13 \pm 4 \mu\text{g L}^{-1}$ was obtained according to 247
DIN32645 (calibration curve method). Prior to analysis, all 248
samples were diluted with a 2% (v/v) HNO₃ solution. The 249
isotopes ⁴⁸Ti and ⁴⁹Ti were always measured simultaneously. 250
However, only the data from ⁴⁹Ti are shown. 251

Miniaturized AF4 with a Multi-Detector Array. 252
Instrumentation and Carrier Liquid. Samples treated with 253
inverse SFE were further separated and analyzed using an 254
asymmetrical flow field-flow fractionation system (AF4) from 255
Postnova Analytics GmbH (AF2000 MF, Postnova Analytics 256
GmbH (PN), Landsberg am Lech, Germany), incorporating an 257
autosampler (PN5300), channel thermostat (PN4020), UV 258
(PN3211) and multi-angle light scattering MALS (PN3621, 21 259
angles) detectors. A miniaturized AF4 cartridge with a tip to tip 260
length of 7 cm (S-AF4-CHA-631, a similar design is further 261
described in ref 18) and incorporating a small 10 kDa 262
regenerated cellulose membrane (20 × 80 mm, Z- 263
AF4_MEM-635–10KD) was used for samples of the model 264
sunscreens and a miniaturized 10 kDa polyether sulfone (PES) 265
membrane (20 × 80 mm, Z-AF4_MEM-631–10KD) for the 266
commercial sunscreens. Furthermore, a 350 μm-thick Mylar 267
spacer was used for all measurements. UV detection was 268
performed at 254 nm, and the measured UV signal was used to 269
correlate concentration with particle size. The MALS detector 270
provided the gyration radius of the particles exiting the 271
miniaturized AF4 (mAF4) separation cartridge (calculated 272
using the random coil model). All presented UV data were 273
collected with the UV detector alone, and all radii of gyration 274
data were determined from the angular dependent light 275
scattering signals obtained via MALS detection. The eluent 276
was prepared using filtrated ultrapure water, to which 0.2% (v/ 277

Table 1. Titanium Dioxide Concentrations Measured after Different Sample Treatments and Subsequent Element-Specific Analysis with Model Sunscreens

	sample preparation: microwave digestion				sample preparation: inverse SFE			
	analytical method: ICP-MS		analytical method: ICP-AES		analytical method: ICP-MS		analytical method: ICP-AES	
	conc (%)	SD	conc (%)	SD	conc (%)	SD	conc (%)	SD
model sunscreen, 0.2% TiO ₂	0.19	0.02	0.21	0.01	0.25	0.03	0.21	0.03
model sunscreen, 1.0% TiO ₂	1.02	0.01	0.99	0.01	1.16	0.05	1.05	0.03
model sunscreen, 5.0% TiO ₂	5.17	0.06	4.95	0.07	5.21	0.06	5.3	0.3

v) filtered NovaChem was added. The injection volume was set to 5 μL for the highly concentrated standard TiO₂ nanoparticles, 10 μL for all model sunscreens and the GarnierCream30 (highest TiO₂ content of the commercial samples), and to 20 μL for all other commercial creams. Prior to analysis, the samples from the model sunscreens were diluted 1:4 in a solution of 0.2% (v/v) NovaChem in ultrapure water and then again sonicated at maximum power (132 kHz) for 15 min. Dilution is necessary to prevent overloading effects, which may cause peak shifts and lead to particle agglomeration. The commercial creams were transferred to a glass vial and sonicated for 30 min without further dilution. The temperature of both the autosampler and the channel thermostat were set to 25 °C. Separations and analysis were performed in quadruplicate ($m = 4$) for each extraction (each cream was sampled in triplicate $n = 3$) and three out of four measurements per extraction were selected for further investigations. To compensate the baseline drift, UV data was corrected by subtracting a blank run signal measured after injection of pure eluent. For the commercial sunscreens, the baseline corrected UV signal was also divided through the original cream weight, eliminating the influence of different sample amounts. The data acquisition and MALS calculations were performed using the AF2000 Control Unit software (Postnova Analytics GmbH, Landsberg am Lech, Germany), and further evaluations (curve subtractions, etc.) were performed using OriginPro 9.1 (OriginLab Corporation, United States).

Elution Profile. An optimized focusing and elution method was developed to ensure reproducible analysis. The focusing step of the selected elution profile was commenced with a 4 min-long injection flow of 0.15 mL min⁻¹ and a cross-flow of 0.30 mL min⁻¹. After a 30 s-long transition time, elution started with a constant cross-flow of 0.30 mL min⁻¹ for an additional 30 s, followed by an exponentially decreasing cross-flow (exponent: 0.2), reaching a final value of 0 mL min⁻¹ after 30 min. The run was completed with a 10 min long rinsing step to check for additional particle release. To ensure a stable signal, the detector flow rate was maintained at 0.35 mL min⁻¹, with the other flows adjusted accordingly.

Determination of Relative Particle Amounts. For the commercial sunscreens, the relative number of particles with a gyration diameter of less than a 100 nm was estimated by integrating the area under the curve of the UV trace between the end of the void peak (6.25 min) and the elution time corresponding to a gyration diameter of 100 nm, as calculated from the MALS measurements.

RESULTS AND DISCUSSIONS

Method Evaluation with Model Sunscreen. Recovery Rate. One of the most relevant figures of merit when separating ENPs from complex matrixes is the recovery rate.³ This was investigated with ICP-AES and ICP-MS for three model sunscreens that were independently treated with both a

standard procedure based on microwave-assisted digestion and inverse SFE.

As shown in Table 1, slightly higher concentrations of TiO₂ were obtained for samples processed with scCO₂, resulting in recovery rates of 104 \pm 4% for the ICP-AES and 115 \pm 17% for the ICP-MS. This apparent increase in concentration is most likely due to solvent evaporation during sample preparation for the inverse SFE treatment: the amount of cream to be processed by scCO₂ is weighed after deposition on the Teflon cartridge, where it is spread into a homogeneous 200 μm thin layer to allow thorough sample penetration. In the time between sample deposition and cartridge weighing, the sample is prone to evaporation due the small amount of cream (about 100 mg) and the large exposed surface (600 mm²). This, in combination with the fact that sunscreens are often tailored for fast solvent evaporation (to promote quick absorption by the skin), may lead to mass losses of up to 10%, shifting the nanoparticle w/w concentration toward higher values. This does not occur when performing acid digestion, thereby explaining the small difference in measured concentrations.

Particle Size Evaluation. Another important factor with regard to the applicability of a sample preparation method is its ability to preserve the size distribution of the nanoparticles and prevent the creation of large agglomerates. To assess this, we used a miniaturized AF4 cartridge to perform rapid size separation and subsequent characterization by different detection techniques.¹⁸ With the miniaturized cartridge and the correspondingly low flow rates, solvent consumption could be reduced to less than 25 mL per run, compared to the 100 mL normally used within the standard analytical channel. The complete run time with the miniaturized channel was 45 min, significantly shorter than what is needed when using standard analytical cartridges, especially when taking into consideration flow presetting and flushing. Besides the three model sunscreens, we also measured the pure nanoparticle dispersion used in their fabrication, allowing direct comparison of the size of the original nanoparticles to those remaining in the simplified matrix after treatment with scCO₂. These data are shown in Figure 2, where the solid lines depict the UV fractograms for the different model sunscreens and the black dashed line shows the comparative UV data for the original nanoparticle suspension. The red dashed line shows the averaged MALS curve for the pure dispersion, which is in good agreement with the corresponding curves for the model sunscreens. Peak positions in the different fractograms are in close correspondence with only a small shift of the main peak for the treated particles toward larger sizes. These slight shifts are almost certainly due to aggregation. Nevertheless, because larger particles scatter light strongly, even small amounts of aggregates would result in higher signals. Accordingly, the elugrams indicate the presence of only minor aggregates. The very small peak occurring between 15 and 20 min most likely originates from other cream excipients being slightly active in

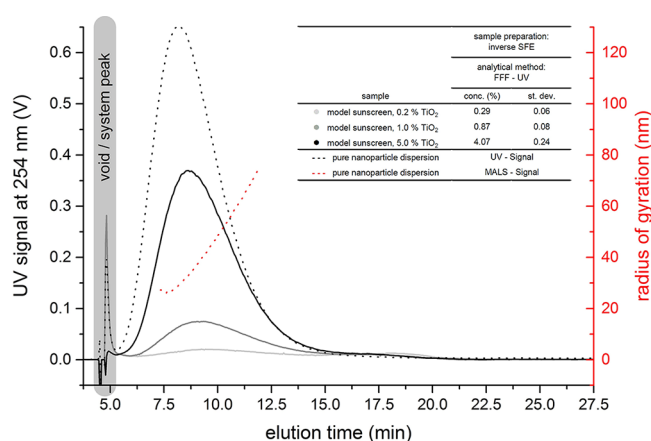


Figure 2. Fractograms of the three scCO₂ treated model sunscreens. In addition, the UV signal and calculated radius of gyration from the MALS detector of the pure nanoparticle dispersion are shown, confirming the excellent correspondence between the size distributions from the original particles and those extracted from the complex sunscreen matrix.

been shown previously that organic acids can form in the presence of water and scCO₂ and that such acids can diminish the suspension stability of TiO₂ nanoparticles.^{31,32} The treatment with inverse SFE could therefore lead to a modification in the nanoparticle's surfactant properties, which would result in particle agglomeration. These larger aggregates are unlikely to be completely ionized by the ICP ion source, thereby resulting in lower recoveries at the detector. Furthermore, the different measurement process parameters of ICP-MS and ICP-AES such as speed and sample uptake could also yield more rapid precipitation for highly aggregated particles in the case of ICP-MS, leading to lower recovery rates compared to those of ICP-AES.³³

To further investigate this issue, we performed additional measurements where sunscreens processed using inverse SFE were further treated with microwave-assisted digestion prior to analysis with element-specific tools. This additional mineralization step should allow the proper ionization of all the TiO₂ left after treatment with supercritical CO₂, clarifying whether particles were lost during inverse SFE treatment or not.

The data in Table 3 report the recovery rates for the three nanoparticle-containing commercial samples after employing

Table 3. Recovery Rates of the Three Commercial Products Containing TiO₂ Nanoparticles^a

	sample preparation: inverse SFE		sample preparation: iSFE + microwave digestion	
	analytical method: ICP-MS (%)	analytical method: ICP-AES (%)	analytical method: ICP-MS (%)	analytical method: ICP-AES (%)
NC15	52 ± 16	79 ± 4	106 ± 14	95 ± 6
NC30	37 ± 20	78 ± 28	110 ± 8	90 ± 8
GC30	44 ± 7	80 ± 15	68 ± 10	78 ± 12

^aAbbreviations: NC15, NiveaCream15; NC30, NiveaCream30; GC30, GarnierCream30.

only inverse SFE and after processing creams with inverse SFE followed by microwave-assisted digestion. As can be seen, the obtained recovery values are higher in the latter case, indicating the issue is not a result of particle loss during inverse SFE but rather due to incomplete ionization of the gently treated samples.

Particle Size Evaluation. The aforementioned drop in recovery rate may pose an issue for quantitative measurements. However, one significant advantage of inverse SFE over microwave-assisted digestion is its capability to preserve nanoparticles during pretreatment, thus allowing further investigation. In the case of microwave-assisted digestion, the metals are fully solubilized, thereby destroying their particulate nature and preventing further investigation. On the contrary,

the selected UV absorption range, as previously noted¹⁶ and through additional ICP-MS measurements (data not shown). Overall, however, the data clearly indicate excellent preservation of the size distribution of the particles between the pure and treated samples.

Method Evaluation with Commercial Sunscreens.

Recovery Rate. After the sample preparation efficiency of inverse SFE was thoroughly tested on model sunscreens, the method was applied to commercial sunscreens. For these tests, we purchased a set of five sunscreens and processed them using the same protocol that was used for the three model sunscreen formulations, in addition to microwave-assisted digestion and the treatment with supercritical CO₂ (Table 2). Significantly, the TiO₂ concentrations, determined after microwave digestion with the two methods, are in good agreement, allowing an accurate estimation of the TiO₂ content in the commercial formulations. The values for the CoopCream50 and the SherpaSpray30 (the two creams sold as being TiO₂-free) gave signals consistently below the detection limit of the respective analytical technique.

An interesting result was observed when using elemental techniques to determine the TiO₂ concentration after inverse SFE. The value obtained with ICP-AES was approximately 79% of the initial concentration, with little variation among different screens. Conversely, ICP-MS data estimated 52, 37, and 44% of the corresponding initial values. The reduced recovery rate for the commercial sunscreens may indicate a severe loss of TiO₂ during sample preparation with inverse SFE. However, it has

Table 2. Titanium Dioxide Concentrations Measured after Different Sample Treatments and Subsequent Element-Specific Analysis for Five Commercial Sunscreens

	sample preparation: microwave digestion				sample preparation: inverse SFE			
	analytical method: ICP-MS		analytical method: ICP-AES		analytical method: ICP-MS		analytical method: ICP-AES	
	conc (%)	SD	conc (%)	SD	conc (%)	SD	conc (%)	SD
NiveaCream15	0.99	0.03	0.92	0.01	0.5	0.2	0.72	0.03
NiveaCream30	1.9	0.2	1.76	0.08	0.7	0.4	1.4	0.5
GarnierCream30	3.4	0.2	3.0	0.2	1.5	0.2	2.4	0.4
CoopCream50	<LoD		<LoD		<LoD		<LoD	
SherpaSpray30	<LoD		<LoD		<LoD		<LoD	

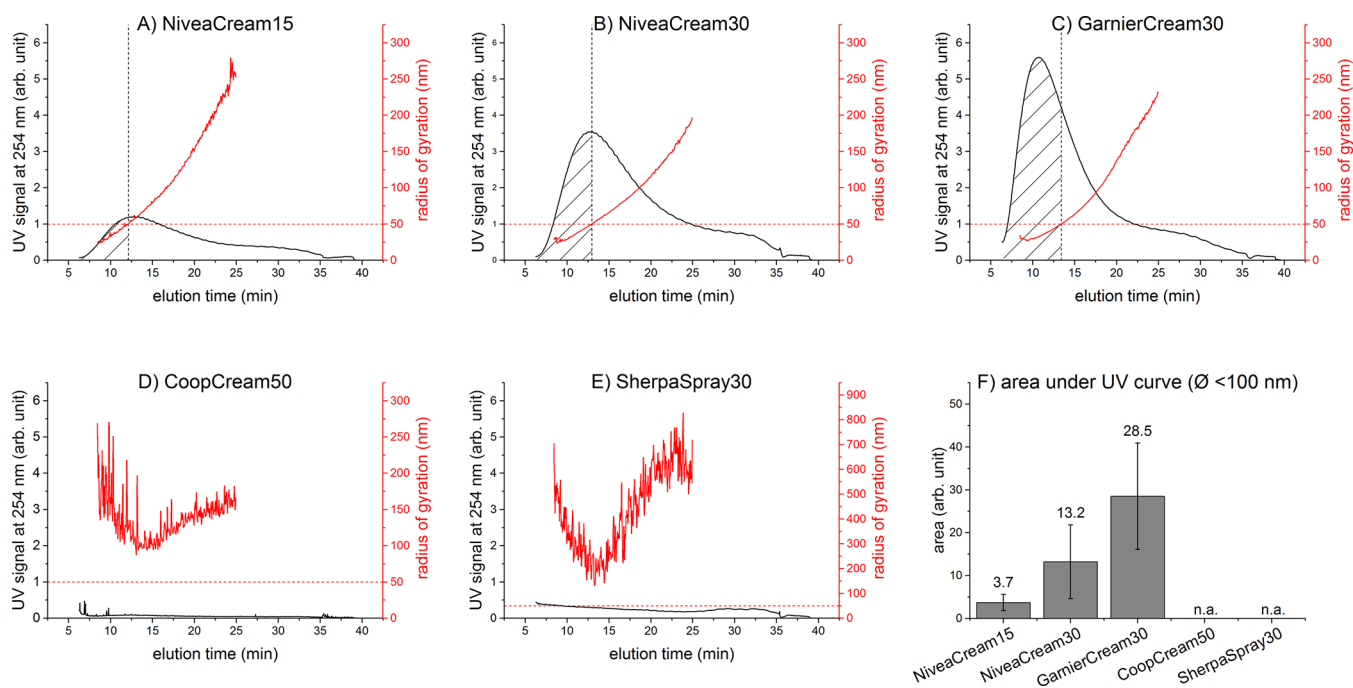


Figure 3. (A–E) Fractograms reporting the UV signal (black) and the calculated radius of gyration (red) for five commercial creams. (A–C) The first three creams clearly contain nanoparticles over a wide size range, whereas the latter two creams (D and E) show limited UV absorption and no detectable particles in the nanoscale range (and an incoherent sizing curve due to low scattering signal). Subset F shows the relative area under the UV curve before the threshold of an averaged gyration radius of 50 nm (dashed area in A–C). Error bars depict standard deviations ($n = 9$).

Figures 3A–E show the fractograms of resuspensions from the commercial samples treated with supercritical CO₂. In the case of subset A–C, both UV and MALS data show a continuous signal, in line with actual increase in concentration or size and similar to that observed with the model samples. These three creams list, as previously noted, TiO₂ nanoparticles as one of their ingredients. The creams not listing TiO₂ or any kind of nanoparticles show minimal UV absorption. In those cases, the MALS detector is unable to determine a cohesive sizing curve, as the low scattering signal is insufficient to allow fitting to the model (Figures 3D and E). The small UV signal could be due to excipients other than TiO₂ nanoparticles, which may not have been fully removed by inverse SFE and which are also active in the selected UV absorption range.

Figure 3F shows the area under the UV curve for all commercial samples up to a determined diameter of gyration of 100 nm. As the MALS curves for the two later creams, CoopCream50 and SherpaSpray30, never exceed this threshold, no values could be calculated for those samples. Due to the unknown UV absorbance of other cream components and the relatively large deviations between different runs on the same sample (see error bars in Figure 3F), these data cannot be used for an accurate determination of TiO₂ content. Nevertheless, the trends are consistent with the results obtained from the element-specific detection techniques, indicating that the method is eminently suitable for a preliminary screening of TiO₂ particle content.

Inconsistencies in the recovery rate of ICP-MS compared to ICP-AES, as seen here, are generally not uncommon and have been shown to become more severe if different sample pretreatment are employed.³³ In addition to the variations between the different creams, we observed significant deviations between different aliquots of the same sample. This is also indicated by the standard deviations and percentage

ranges shown in Tables 2 and 3 as well as the error bars of Figure 3F, which demonstrate the challenging nature of the analysis of the commercial creams compared to model sunscreens. Results could be improved by extending sample preparation by post-treatment stabilization of the sample, as suggested by Wagner.³ These additional procedures would stabilize the particles and therefore the analytical outcome as a whole as well as optimize method performance for a specific combination and purpose such as iSFE-mAF4-UV-MALS for the determination of TiO₂ particle size distributions or microwave-assisted digestion of the native creams followed by ICP-AES or ICP-MS for the determination of the overall TiO₂ content.

CONCLUSIONS

In this study, we present a novel approach for the analysis of TiO₂ nanoparticles in commercial sunscreens that comprises two analytical procedures. In a first step, inverse SFE was used to gently remove sunscreen matrix components, resulting in dried sunscreen strips containing residual TiO₂ nanoparticles, which were easily redispersible. With recovery rates ranging between 68 and 110%, ICP-MS and ICP-AES measurements of the commercial sunscreen samples before and after treatment confirmed no significant loss of TiO₂ nanoparticles during the sample preparation process.

In a second step, after redispersion in an aqueous solvent, the TiO₂ nanoparticles were characterized using mAF4 hyphenated with UV and MALS detection. This approach allowed for fast and reliable fractionation and sizing of the TiO₂ nanoparticles and thus an unambiguous determination of the presence or absence of TiO₂ particles in commercial sunscreens. The obtained results were in agreement with the data from the element-specific tools and with the label indications for all investigated creams.

514 The combination of inverse SFE with miniaturized AF4
515 proved to be a highly powerful and efficient tool for the
516 verification of the nanocontent of commercial sunscreens. Due
517 to its wide applicability, this analytical approach is not solely
518 limited to sunscreens but could also be used with cosmetic
519 formulations containing other inorganic particles such as zinc
520 oxide, ceria, or silver. Furthermore, the method is fully in line
521 with the increasingly compelling demand for environmentally
522 friendly analytical methods due to the use of a mild solvent
523 (scCO₂) in combination with reduced consumption of eluent.
524 In addition, as a pure sample preparation method, inverse SFE
525 could potentially be applied to other analytical techniques for
526 the investigation of nanoparticles in complex cosmetic matrixes,
527 including electron microscopy, nanoparticle tracking analysis or
528 single particle ICP-MS. This renders inverse SFE a universal
529 tool for the preparation of cosmetic samples, significantly
530 contributing to the quest for routine analytical methods for the
531 verification of European Union nanoparticle labeling require-
532 ments.¹

533 ■ AUTHOR INFORMATION

534 Corresponding Author

535 *E-mail: science@davidmueller.ch.

536 ORCID

537 David Müller: 0000-0003-1914-3768

538 Andrew deMello: 0000-0003-1943-1356

539 Present Address

540 ¹D.M.: Mythenstrasse 2, 6003 Luzern, Switzerland.

541 Notes

542 The authors declare no competing financial interest.

543 ■ ACKNOWLEDGMENTS

544 This work was supported by the European Commission
545 Seventh Framework Programme (Project SMART-NANO,
546 NMP4-SE-2012-280779).

547 ■ ABBREVIATIONS

548 CO ₂	carbon-dioxide
549 scCO ₂	supercritical CO ₂
550 AF4	asymmetrical flow field-flow fractionation
551 mAF4	miniaturized AF4
552 SFE	supercritical fluid extraction
553 iSFE	inverse SFE
554 MALS	multiangle light scattering
555 ICP-AES	inductively coupled plasma atomic emission spec- trometer
556 ICP-MS	inductively coupled plasma mass spectrometer

558 ■ REFERENCES

- 559 (1) EC. *Report No. 342*; Off. J. Eur. Union: 2009, pp 59–209.
- 560 (2) Calzolari, L.; Gilliland, D.; Rossi, F. *Food Addit. Contam., Part A*
561 **2012**, *29* (8), 1183–1193.
- 562 (3) Wagner, S.; Legros, S.; Loeschner, K.; Liu, J.; Navratilova, J.;
563 Grombe, R.; Linsinger, T. P. J.; Larsen, E. H.; von der Kammer, F.;
564 Hofmann, T. *J. Anal. At. Spectrom.* **2015**, *30*, 1–11.
- 565 (4) von der Kammer, F.; Ferguson, P. L.; Holden, P. A.; Masion, A.;
566 Rogers, K. R.; Klaine, S. J.; Koelmans, A. A.; Horne, N.; Unrine, J. M.
567 *Environ. Toxicol. Chem.* **2012**, *31* (1), 32–49.
- 568 (5) Contado, C.; Pagnoni, A. *Anal. Methods* **2010**, *2* (8), 1112–1124.
- 569 (6) Dan, Y.; Shi, H.; Stephan, C.; Liang, X. *Microchem. J.* **2015**, *122*,
570 119–126.
- 571 (7) Nischwitz, V.; Goenaga-Infante, H. *J. Anal. At. Spectrom.* **2012**, *27*
572 (7), 1084.

- (8) Tadjiki, S.; Assemi, S.; Deering, C. E.; Veranth, J. M.; Miller, J. D. *J. Nanopart. Res.* **2009**, *11* (4), 981–988. 573
- (9) Plathe, K. L.; Von Der Kammer, F.; Hassellöv, M.; Moore, J.; 574
Murayama, M.; Hofmann, T.; Hochella, M. F. *Environ. Chem.* **2010**, *7* 575
(1), 82–93. 576
- (10) Dunford, R.; Salinaro, A.; Cai, L.; Serpone, N.; Horikoshi, S.; 577
Hidaka, H.; Knowland, J. *FEBS Lett.* **1997**, *418* (1–2), 87–90. 578
- (11) Lewicka, Z. a.; Benedetto, A. F.; Benoit, D. N.; Yu, W. W.; 579
Fortner, J. D.; Colvin, V. L. *J. Nanopart. Res.* **2011**, *13* (9), 3607–3617. 580
- (12) Capello, C.; Fischer, U.; Hungerbuhler, K. *Green Chem.* **2007**, *9*, 581
927–934. 582
- (13) Moore, W. N.; Taylor, L. T. *J. Pharm. Biomed. Anal.* **1994**, *12* 583
(10), 1227–1232. 584
- (14) Messer, D. C.; Taylor, L. T. *Anal. Chem.* **1994**, *66* (9), 1591– 585
1592. 586
- (15) Almodovar, R. A.; Rodriguez, R. A.; Rosario, O. *J. Pharm.* 587
Biomed. Anal. **1998**, *17*, 89–93. 588
- (16) Müller, D.; Cattaneo, S.; Meier, F.; Welz, R.; de Vries, T.; 589
Portugal-Cohen, M.; Antonio, D. C.; Cascio, C.; Calzolari, L.; Gilliland, 590
D.; de Mello, A. *J. Chromatogr. A* **2016**, *1440*, 31–36. 591
- (17) M-M, P.; Siripinyanond, A. *J. Anal. At. Spectrom.* **2014**, *29* (10), 592
1739–1752. 593
- (18) Müller, D.; Cattaneo, S.; Meier, F.; Welz, R.; DeMello, A. *Front.* 594
Chem. **2015**, *3* (July), 45. 595
- (19) Scalia, S.; Simeoni, S. *Chromatographia* **2001**, *53*, 490–494. 596
- (20) Kaupp, G. *Angew. Chem., Int. Ed. Engl.* **1994**, *33* (14), 1452– 597
1455. 598
- (21) Ndiomu, D. P.; Simpson, C. F. *Anal. Chim. Acta* **1988**, *213*, 600
237–243. 601
- (22) Hawthorne, S. B. *Anal. Chem.* **1990**, *62* (11), 633–642. 602
- (23) Engelhardt, H.; Zapp, J.; Kolla, P. *Chromatographia* **1991**, *32* 603
(11/12), 527–537. 604
- (24) Reverchon, E.; De Marco, I. *J. Supercrit. Fluids* **2006**, *38* (2), 605
146–166. 606
- (25) Goto, M.; Sato, M.; Hirose, T. *J. Chem. Eng. Jpn.* **1993**, *26*, 401– 607
407. 608
- (26) Roy, B. C.; Goto, M.; Hirose, T. *Ind. Eng. Chem. Res.* **1996**, *35* 609
(2), 607–612. 610
- (27) Peker, H.; Srinivasan, M.; Smith, J.; McCoy, B. *AIChE J.* **1992**, 611
38 (5), 761–770. 612
- (28) Tello, J.; Viguera, M.; Calvo, L. *J. Supercrit. Fluids* **2011**, *59* 613
(2011), 53–60. 614
- (29) Lee, M. R.; Lin, C. Y.; Li, Z. G.; Tsai, T. F. *J. Chromatogr. A* 615
2006, *1120* (1–2), 244–251. 616
- (30) Scalia, S. *J. Chromatogr. A* **2000**, *870* (1–2), 199–205. 617
- (31) Pettibone, J. M.; Cwiertny, D. M.; Scherer, M.; Grassian, V. H. 618
Langmuir **2008**, *24* (13), 6659–6667. 619
- (32) Choi, Y. S.; Nešić, S. *Int. J. Greenhouse Gas Control* **2011**, *5* (4), 620
788–797. 621
- (33) Iwashita, A.; Nakajima, T.; Takanashi, H.; Ohki, A.; Fujita, Y.; 622
Yamashita, T. *Fuel* **2006**, *85* (2), 257–263. 623